Complex-Wall Effect on Propagation Characteristics and MIMO Capacities for an Indoor Wireless Communication Environment

Zhengqing Yun, *Member, IEEE*, Magdy F. Iskander, *Fellow, IEEE*, and Zhijun Zhang, *Member, IEEE*

***Abstract*—The effects of complex wall structures on the characteristics of fading and the capacity of multi-input multi-output (MIMO) wireless communication systems for some typical indoor propagation environments are investigated. Two cases of wall structures are examined in this paper. In the first case, the walls are considered to be homogenous solid slabs, while, in the second case, the walls are assumed to be of complex structures. A two-dimensional finite difference time domain method is employed to calculate the electric field distributions, and then, the local mean power, the Rician K factor, and the MIMO capacity are calculated and analyzed. It is found that the patterns of the local mean power distributions are different for the two wall-structure cases. As for the small-scale fading, it is shown that the Rician K factors for the two cases may be different by 5 dB. The resulting values of MIMO capacities are also quite different and are less than the ideal cases, where the elements of the transfer (H) matrix are assumed to be zero-mean Gaussians with unit variance. We also investigate the cases where complex walls are replaced by effective slab walls. It is found that complex walls cannot be appropriately characterized by simple effective slab walls as considerable difference exists between the two cases.**

I. Introduction

With the rapid deployment of wireless communication systems and the advent of multi-input multi-output (MIMO) systems, accurate propagation characterization is needed for coverage, optimal site design, calculation of system capacity, and so on. To ensure an accurate propagation prediction, it is important to develop accurate models for the propagation environments, including the geometry and electrical properties of building walls and other objects involved. Usually, a wall in a building is approximated by an interface of two different materials, as in the outdoor cases, and/or homogenous solid slabs when transmission is considered (for indoor and/or outdoor to indoor cases). It is also common to assume that walls are infinitely thin in determining the transmitted ray trajectory when ray-tracing method is used. Recently, some investigations have been made in characterizing the effects of wall thickness, dielectric parameters, and complex geometries of walls on the accuracy of propagation prediction models [1]–[6]. It was reported in [6] that the delay spread is sensitive to the building dielectric parameters. The effects of complex walls like those shown in Fig. 1(b) on path loss prediction are most interesting because resonance, i.e., total transmission, may occur at some specific angles of incidence. It is reported that the path loss is different by as much as 8–10 dB between solid walls and those of complex structures in a simple outdoor case [1]. The complex walls can be equivalently represented by three uniform layers using the homogenization method. The dielectric parameters of the first and the third layers are identical and constants, and equal to the value of the wall material, while the dielectric parameter of the mid-layer varies with the angle of incidence. The complex structures will give more complicated multipaths and will affect the fading characteristics and capacity of MIMO systems. It should be noted that most studies on MIMO systems and the estimation of their capacity have been theoretical and involved simplified assumption regarding propagation environments [7]–[14], although some experiments have been carried out [15]–[17]. No investigation has been carried out for the effect of realistic wall structures on MIMO capacities to the authors' knowledge.

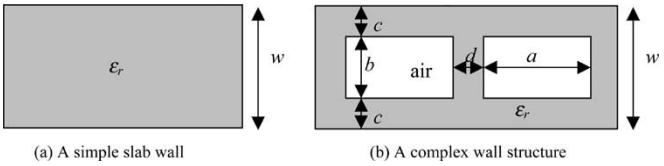

Fig. 1. Simple slab walls and complex walls used in the simulation. (a) Simple slab wall. (b) Complex wall structure.

In this paper, we present the results of a study on the effects of complex wall structures on the fading properties and the capacity of MIMO systems. Calculations are made using an finite difference time domain (FDTD) method that can provide more detailed (high resolution) and accurate results than a ray-tracing approach, as the complex wall structures are involved. First, a case where walls are simulated by slabs is calculated as a reference. Then, complex walls with the same thickness are used and the electric field distribution in the propagation environment is calculated. The local mean power distribution, the small-scale fading characteristics, and the MIMO capacities are then obtained and compared for the two cases of wall structures. It is found that the patterns and coverage of the local mean power distributions of the two cases are different and the K factors for the two cases are different by as much as 5 dB. The calculated MIMO capacities are also quite different and are less than those calculated using the ideal cases where the elements of H matrix are assumed zero mean unit variance Gaussians. When complex walls are replaced by effective slab-walls, the various results are calculated and compared with the slab and complex wall cases. It is found that the

Manuscript received December 20, 2002; revised May 1, 2003.

The authors are with the Hawaii Center for Advanced Communication, College of Engineering, University of Hawaii at Manoa, Honolulu, HI 96822 USA.

Digital Object Identifier 10.1109/TAP.2004.825691

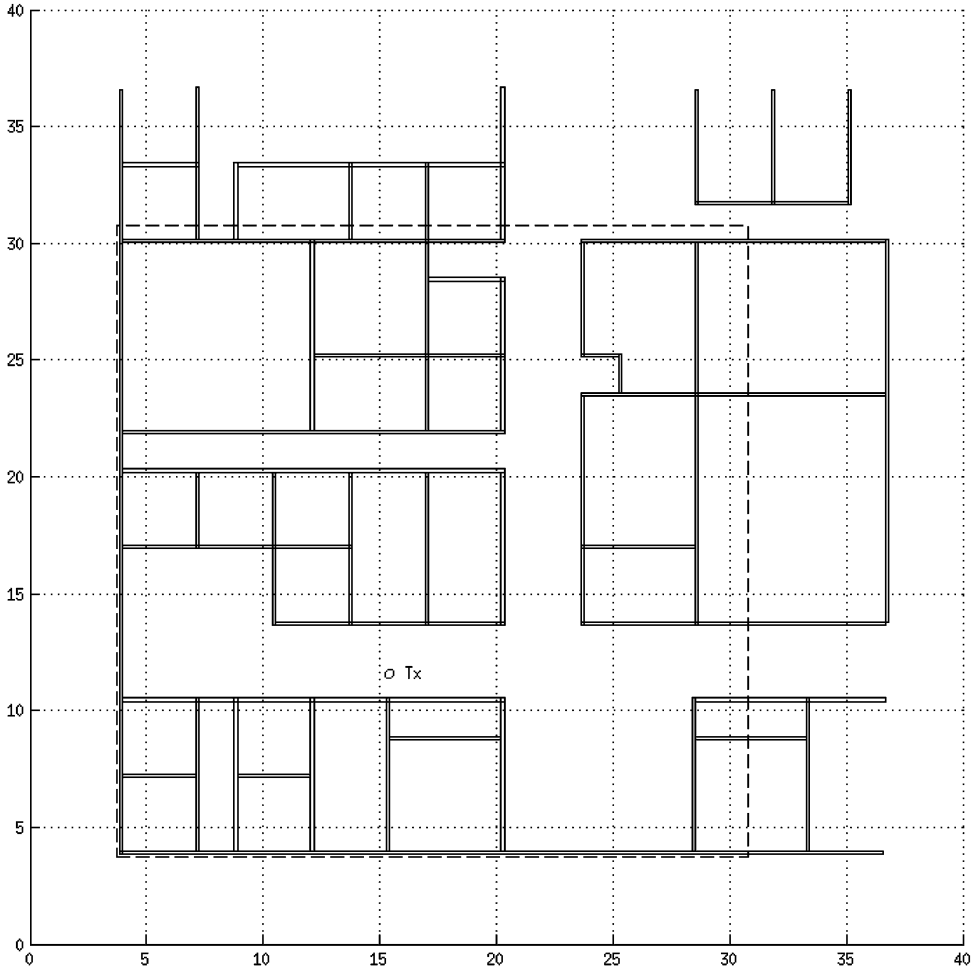

Fig. 2. FDTD model for a floor plan in a building. The whole FDTD model has a dimension around 40 × 40 m. The fields in the dashed rectangle (around 27 × 27 m) will be analyzed. All dimensions are in meters.

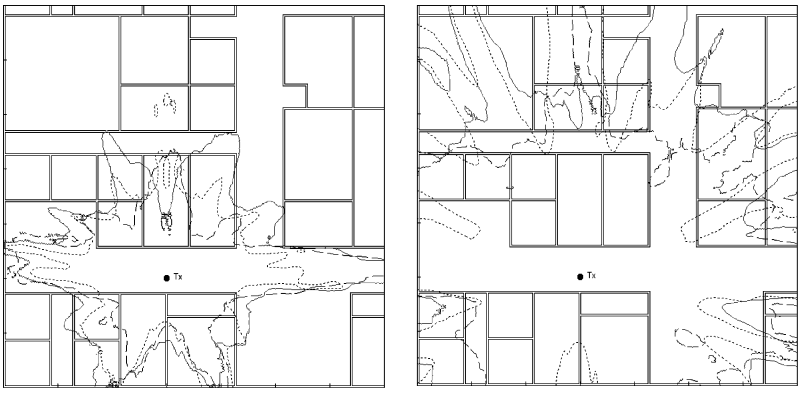

(a) Power contours (-5 dB) (b) Power contours (-10 dB)

Fig. 3. Comparisons of equal-power patterns between (solid line) the complex, (dashed line) slab walls, and (dotted line) effective walls. (a) For −5-dB power contours. (b) For −10-dB power contours.

effective wall structures behave more like slabs walls instead of complex walls, which means that simple effective wall structures do not represent the complex walls very well.

II. Finite Difference Time Domain Modeling

We focus our study on the comparison of simple and complex walls with the geometries shown in Fig. 1(b). Although other complex geometries [4] may have been considered, the one shown in Fig. 1(b) serves as a representative example that will illustrate impact of wall structures on the characterization of a propagation environment. The reflection and transmission properties of this kind of wall can be analyzed using the homogenization method [1]. It is shown in [1] and [2] that resonance effect may occur for some angles of incidence and at some frequencies and the reflected and transmitted powers can be very

TABLE I
PERCENT COVERAGE OF THE POWER CONTOURS

Relative Power levels (dB)		0	> -5	> -10	> -15
Coverage (%)	Complex walls	3.17	28.51	73.54	99.64
	Slab walls	2.23	19.68	57.65	88.92
	Effective walls	2.44	19.34	67.63	97.83
Coverage Ratios	Complex / slab	1.4	1.4	1.3	1.1
	Complex / effective	1.3	1.5	1.1	1.0

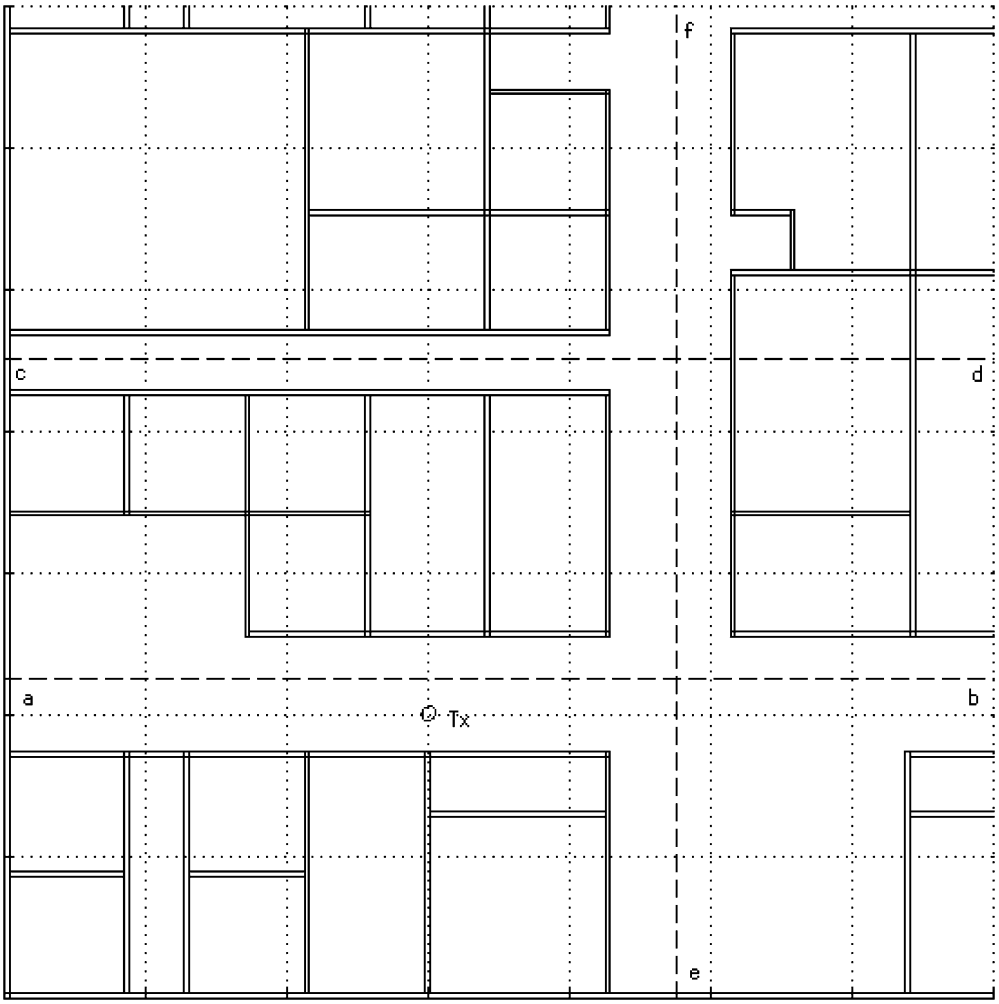

Fig. 4. Three lines on which small scale fading characteristics are examined.

different from those calculated based on the assumption of the solid slab walls. The dimensions of the walls shown in Fig. 1 are $w = 13.4715$ cm, $a = w$, $b = 9.6225$ cm, and $c = d = 1.9245$ cm. The frequency is assumed to be 900 MHz with wavelength in air equal to $\lambda_0 = 1/3$ m. The relative permittivity of the material ϵ_r is equal to 3.0 and the wavelength in the material is thus approximately equal $\lambda_\epsilon = \lambda_0/\sqrt{3} = 19.245$ cm. The conductivity of the material is $\sigma = 1.95 \times 10^{-3}$ S/m.

This paper employs the FDTD method to accurately characterize the different effects of simple and complex walls on the power distribution, Rician K factor, and the MIMO capacity. A two-dimensional (2-D) FDTD code is used to simulate the electric field distributions. To make things more realistic, the floor layout of a real building is employed, as shown in Fig. 2. The position of the transmitter is also shown in the figure. The total dimension is around 30 $\times$ 30 m. A square FDTD grid is used with a cell size equal to 1/10 of the wavelength in material λ_ε.

First, the solid slab walls are assumed. The FDTD simulation gives the electric field distribution in the whole region. Second, the FDTD simulation is carried out when slab walls are replaced by complex walls and the field distribution is obtained. Third, the complex walls are substituted by their effective walls, and the field distribution is again calculated. The power distribution can be calculated as the square of the magnitude of the electric field.

III. CALCULATION OF MEAN POWER, RICIAN FACTOR, AND MIMO CAPACITY

For the calculation of the local mean signal strength, several methods exist in the literature [18] and [19]. Valenzuela *et al.* use the average (in watts) of a large number of the measured

values while rotating transmit and/or receive antennas over a horizontal circle with radius equal to several wavelengths [17]. In this paper, we first calculate the electric field distribution in the region of interest, and this gives the complex electric fields at each FDTD cell. Since the cell size is about 1/17 of the wavelength in the air, the obtained fields samples are of high resolution. The local mean power at a point p is calculated using the average values over a square centered at p and with side length of several wavelengths $(6\lambda_0)$. We believe that this will be more accurate than the average value over a circle or a line segment. The local mean power at a point p is thus defined as

$$E_p\left(a^2\right) = \frac{1}{N^2}\sum_{i,j=1}^{N} a^2(i,j) \tag{1a}$$

where E stands for expectation (average values), N^2 is the number of the FDTD cells, and $a(i,j)$ is the signal strength at cell (i,j). The local mean signal strength (the electric field) can be calculated similarly as

$$E_p(a) = \frac{1}{N^2}\sum_{i,j=1}^{N} a(i,j). \tag{1b}$$

The small-scale fading can be characterized by the Rician distribution [20] that represents the more general case with possible dominant rays [e.g., in line-of-sight (LOS) regions]. The envelop distribution of the signal strength a can be written as

$$f(a) = \frac{a}{\sigma^2}\exp\left(-\frac{a^2+A^2}{2\sigma^2}\right) I_0\left(\frac{Aa}{\sigma^2}\right) \quad 0 \le a \le \infty \tag{2}$$

where $\sigma^2 = E(|a|^2)$ is the average power, A is the peak amplitude of the dominant signal, and I_0 is the modified Bessel function of the first kind with zero order. Usually, the Rician distribution is characterized by the K factor that is defined as the ratio of dominant power to the scattered power [20], hence

$$K = \frac{A^2}{2\sigma^2} \text{ or}$$
$$K\,(\text{dB}) = 10\log\frac{A^2}{2\sigma^2}\ \text{dB}. \tag{3}$$

A larger K value means a stronger dominant power and usually happens in the LOS or equivalent cases. It also means that the fading is less severe in this case. The envelop distribution (2) can then be rewritten in terms of K factor as [21]

$$f(a) = \frac{2a(K+1)}{\sigma^2}\exp\left(-K - \frac{(K+1)a^2}{\sigma^2}\right) \times I_0\left(2a\sqrt{\frac{K(K+1)}{\sigma^2}}\right)$$
$$0 \le a \le \infty.$$

The K factor can be calculated by solving the following equation [22] when the electric field distribution is known:

$$\frac{E[a]}{\sqrt{E[a^2]}} = \sqrt{\frac{\pi}{4(K+1)}}\exp\left(-\frac{K}{2}\right) \times\left[(K+1)I_0\left(\frac{K}{2}\right) + KI_1\left(\frac{K}{2}\right)\right] \tag{4}$$

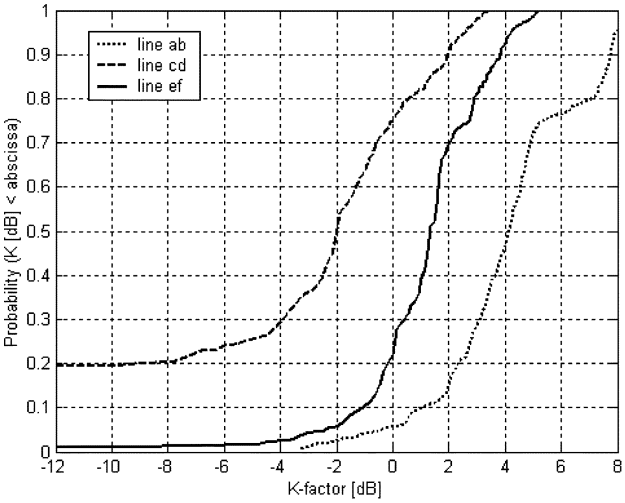

(a) Results for complex walls

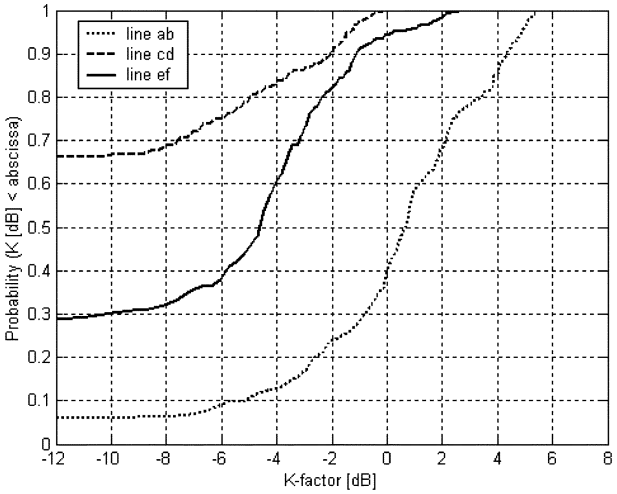

(b) Results for slab walls

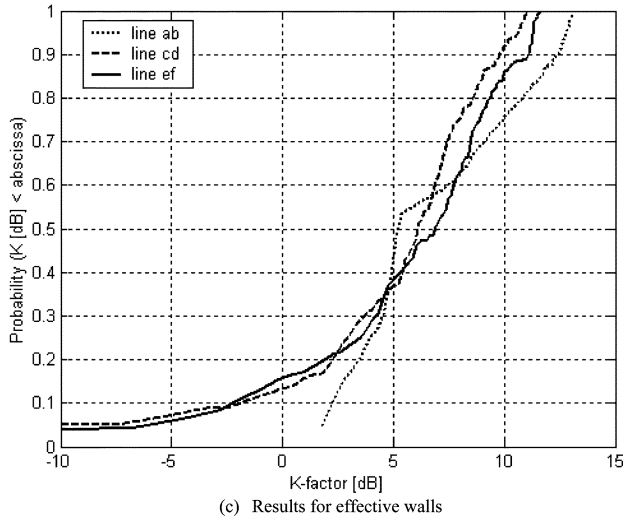

(c) Results for effective walls

Fig. 5. Cumulative density functions of the K and the mean values of K along the designated three lines ab, cd, and ef, as shown in Fig. 4. (a) Results for complex walls. (b) Results for slab walls. (c) Results for effective walls.

where $E(a)$, and $E(a^2)$ are average values of the field magnitude and power, respectively. It should be noted that when $K = 0$, the Rician distribution becomes the Rayleigh distribution, which corresponds to the case with no dominant rays (e.g., in non-LOS regions).

TABLE II
COMPARISON OF THE AVERAGE AND STANDARD DEVIATION (STD) OF K FACTORS ALONG THREE LINES

Lines		*ab*		*cd*		*ef*	
		Average (dB)	STD (dB)	Average (dB)	STD (dB)	Average (dB)	STD (dB)
Complex wall (A)		4.18	2.50	-1.20	2.54	1.35	1.93
Slab wall (B)		0.72	2.87	-4.17	2.63	-3.56	2.67
Effective wall (C)		6.81	3.54	5.70	3.62	5.95	4.29
Average difference	A–B	3.46	-	2.97	-	4.91	-
	A–C	-2.63	-	-6.90	-	-4.60	-

The MIMO capacity calculation can be done if the H matrix is found. Assume, without loss of generality, the number of transmit and receive antennas are assumed to be the same and equal to n. The H matrix is expressed as follows:

$$H(n,n) = \begin{pmatrix} h_{11} & h_{12} & \dots & h_{1n} \\ h_{21} & h_{22} & \dots & h_{2n} \\ \vdots & \vdots & \vdots & \vdots \\ h_{n1} & h_{n2} & \dots & h_{nn} \end{pmatrix}. \quad (5)$$

The element h_{ij} $(i,j = 1,2,\dots,n)$ in the H matrix is the received signal (complex valued) of the receive antenna i from transmitter j. To determine the H matrix using FDTD method, we first calculate the complex electric field distribution for each transmitter antenna, Tx_j $(j = 1,2,\dots,n)$. Then, the received complex field at receive antenna Rx_i $(i = 1,2,\dots,n)$ due to the jth transmitter can be easily determined by picking up the field at the receive antenna's location in the field distribution generated by the jth transmit antenna. The capacity $C(n,n)$ is then calculated as

$$C(n,n) = \log_2 \det\left[I_n + \frac{\rho}{n} HH^*\right] \text{ (bps/Hz) [13]} \quad (6)$$

where, det means determinant, I_n is the identity matrix, * means transpose conjugate, and ρ is the signal-to-noise ratio.

In this paper, we consider only linear antenna arrays (both for transmit and receive antennas) and assume the distance between two neighboring antennas (for both transmit and receive antennas) is equal to half the wavelength.

IV. RESULTS

A. Local Mean Power Distributions

First, the patterns of the local mean power distribution are calculated and are shown in Fig. 3. It can be seen that the pattern shapes for the two cases of solid slab walls and the complex walls are quite different. The percent areas covered by the power contours are also calculated and listed in Table I. It can be seen from Table I that the difference of coverage areas for the two cases is significant and the complex walls give larger coverage than the slab walls. The coverage for the complex wall case is larger than that for the slab wall case by about 40%.

When the complex walls are replaced by their effective walls, the mean power distribution is also calculated and plotted in Fig. 3 and the coverage percentages are listed in Table I. It is observed from Table I that the coverage for the effective wall structures is similar to that of the slab wall structures in the regions close to the transmitter, while in the regions far away from the transmitter, it is similar to that of the complex wall structures. This can be explained as due to the fact that the effective walls have a smaller relative permittivity ($\varepsilon_{\mathrm{reff}} = 2.0$) than slab walls ($\varepsilon_r = 3.0$), and the energy from the transmitter can propagate longer distances than that for the slab wall cases. It is also clear that the effective walls do not approximate the complex walls well, particularly in the regions close to the transmitter.

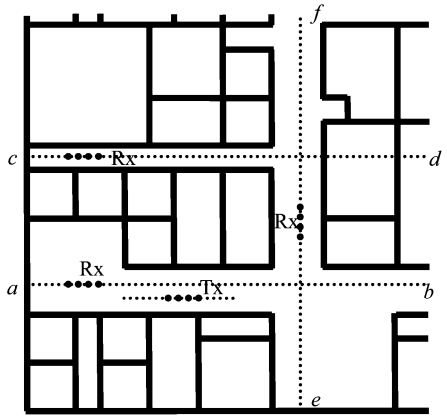

Fig. 6. Linear antenna array geometry for the MIMO capacity calculations. Tx and Rx are the transmit and receive MIMO arrays. (a) Normalized capacity for complex walls. (b) Normalized capacity for slab walls. (c) Normalized capacity for effective walls.

B. Rician K Factors

Second, the Rician K factors are calculated for three lines, ab, cd, and ef, representing the LOS, non-LOS, and a composite region, respectively, as shown in Fig. 4. For each line, values of K factors are calculated for 350 points that are uniformly distributed along the respective line. The distance between two neighboring points is a quarter of wavelength. At each of these 350 points, the mean values of the power $E(a^2)$ and the signal strength $E(a)$ are calculated using (1a) and (1b), respectively. The K values at that point can then be calculated using (4). The cumulative density functions (CDF) of the K values along these three lines are calculated for the complex, slab and effective walls and are shown in Fig. 5.

Table II lists the average values and the standard deviations of the K factors. It can be seen from the figure and the table that, for both cases of complex and slab walls, the K factors have the largest values along line ab and the smallest values along line cd, and the values along line ef are in between. This means that the fading in LOS region (line ab) is less severe than that in the non-LOS region (line cd). It can also be seen that, for each line,

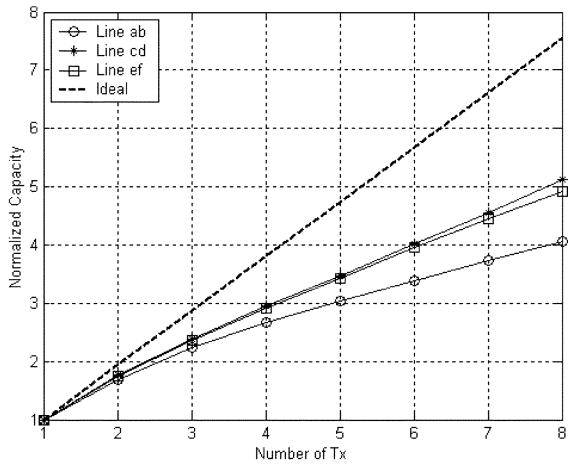

(a) Normalized capacity for complex walls

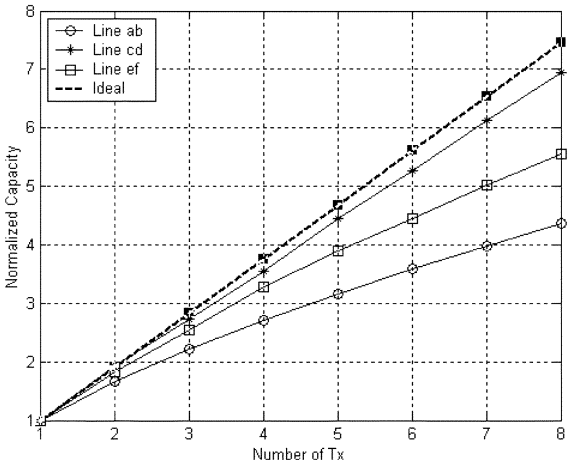

(b) Normalized capacity for slab walls

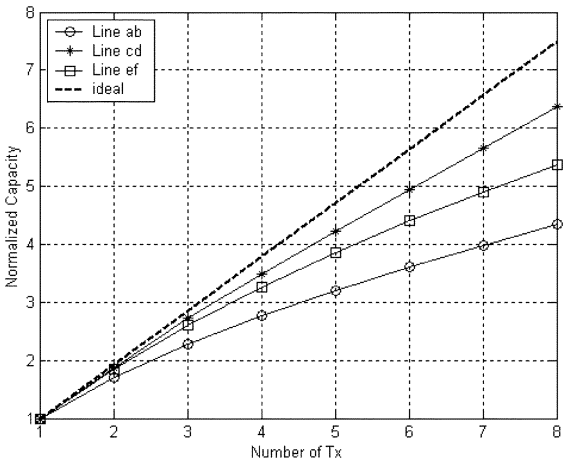

(c) Normalized capacity for effective walls

Fig. 7. Normalized capacities along the three observation lines for the cases of slab, complex, and effective dielectric constant walls. The capacities along a line are normalized to the capacity of single-transmit, single-receive antenna along the line.

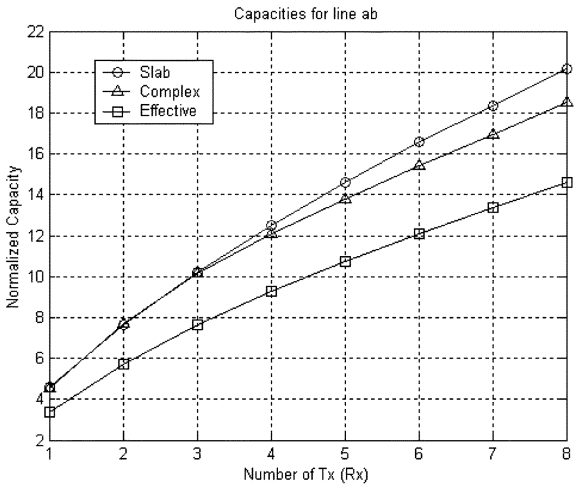

(a) Normalized capacities along line *ab*.

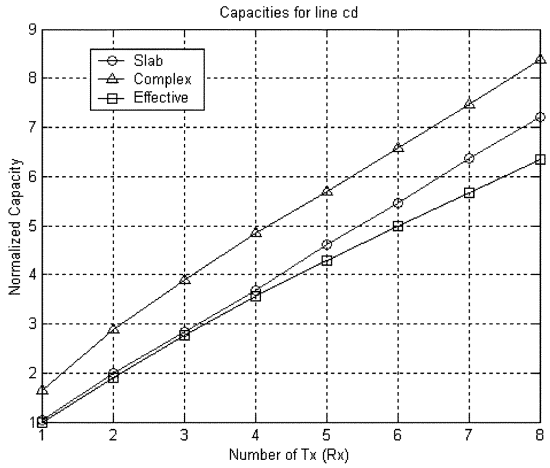

(b) Normalized capacities along line *cd*.

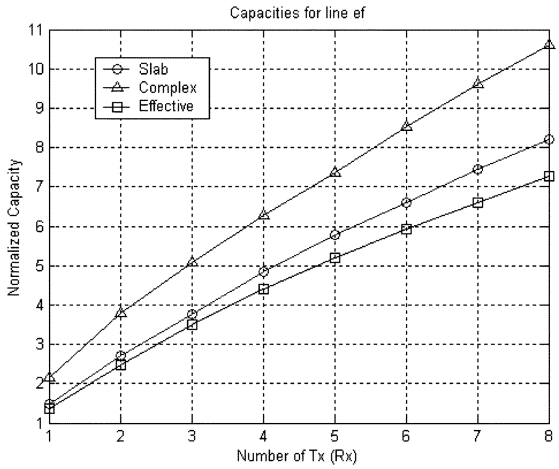

(c) Normalized capacities along line *ef*.

Fig. 8. Normalized capacities along the three lines for the slab, complex, and effective walls. The capacities along the lines are all normalized to the smallest capacity of the single transmit, single receive antenna case, i.e., the effective wall case on line cd. (a) Normalized capacities along line ab. (b) Normalized capacities along line cd. (c) Normalized capacities along line ef.

the fading in the case of complex walls is less severe than that of slab walls. This can be explained by noting that the reflections in the slab wall case are stronger than that for the complex wall case. The differences between the complex and slab wall cases range from around 3 to 5 dB. For the effective walls, the statistics are very different from the complex walls, and the largest value of difference is around 7 dB, larger than the difference between complex and slab walls. The K values for the effective wall cases are the largest because the relative permittivity is small and leads to an environment with less reflection.

C. MIMO Capacities

To examine the MIMO capacity, we fix the locations of the transmit antennas, move the receive antennas along the three

TABLE III
NORMALIZED CAPACITIES

n x n	Line ab			Line cd			Line ef		
	Slab	Complex	Effective	Slab	Complex	Effective	Slab	Complex	Effective
1 x 1	4.61	4.55	3.40	1.04	1.64	1	1.48	2.16	1.35
2 x 2	7.64	7.69	5.73	2.00	2.89	1.91	2.71	3.78	2.48
3 x 3	10.20	10.18	7.65	2.83	3.90	2.76	3.77	5.08	3.50
4 x 4	12.49	12.11	9.28	3.68	4.84	3.56	4.86	6.27	4.41
5 x 5	14.62	13.80	10.72	4.61	5.68	4.29	5.77	7.37	5.20
6 x 6	16.59	15.42	12.07	5.47	6.59	4.99	6.60	8.52	5.92
7 x 7	18.36	16.95	13.35	6.36	7.46	5.66	7.44	9.60	6.61
8 x 8	20.16	18.50	14.58	7.20	8.38	6.33	8.21	10.59	7.26

lines shown in Fig. 4, and calculate the MIMO capacities at each of the uniformly distributed 350 locations (the distance between two neighboring locations is around quarter wavelength as in Section IV-B). Linear antenna arrays are considered in this paper as shown in Fig. 6. The number of transmit antennas are 1, 2,. . ., and 8, and the receive array has the same number of antennas. The average capacities for each transmit-receive pairs along the designated three lines are calculated.

To find how the realistic capacity differs from the ideal capacity calculated by assuming that the elements of the H matrix are zero mean unit variance complex Gaussians, we calculated the capacity increase as a function of the number of transmit (receive) antennas. The average capacities are normalized to the average capacity of the single transmit, single receive antenna system (i.e., $n = 1$). Fig. 7 shows the results for the linear antenna array cases. It can be seen from Fig. 7 that all realistic capacities increase at a lower rate than the realistic ones with the increase in the number of antennas. It can also be seen that the capacity along line ab increases at the slowest rate with the increase of number of antennas, the capacity along line cd has the highest rate, and the capacity along line ef has a rate in between. This can be justified by the values of K factors along these lines, i.e., higher K values give lower rates of capacity increase as propagation is dominated by LOS signals.

To compare the capacities among the three wall structures, all the average capacities are normalized to the smallest capacity for a single-transmit, single-receive antenna case (i.e., $n = 1$, effective walls along line cd). Fig. 8 shows the results along lines ab, cd, and ef, and Table III lists the normalized capacity values. From the figure and the table we can observe the following. i) The capacities in the LOS region (line ab) are larger than that in other regions (lines cd and ef). This is mainly due to the fact that the received power level in the LOS region is greater than that in other regions. ii) The capacities for effective wall structures are the smallest in all the cases. This cannot be explained by the received power levels solely. As may be seen from (6), multipath signals and their distribution reflected in the H matrix also impact the values of capacity. For the effective slab wall case, the relative permittivity is lower and this resulted in more uniform field distribution while the complex wall case provided rich multipath environment that resulted in higher capacities at the same received power levels. From Table I, it can be seen that the power distribution for the effective wall structures is similar to that of the slab walls in the region close to the transmit antenna, while in the regions far away from the transmitter, it is similar to that of the complex walls. If the power level plays the sole role, the capacity of effective wall cases should be similar to that of slab wall cases along line ab (region close to the transmitter), while it should be similar to that of complex wall cases along line cd (far-away region). It is obviously not true according to our simulation results. One possible cause is probably the higher uniformity for the electric field distributions for the effective wall structures. This is because the effective walls have smaller relative permittivity and tends to behave more like air and leads to more uniform field distribution. iii) Complex wall structures give higher capacities in the NLOS (line cd) or hybrid regions (line ef). In the LOS region (line ab), the capacity of the complex wall structures is similar to that of the slab wall cases. This indicates that both power level and the field distribution have effect on the values of capacities.

Throughout the presented results, walls of complex structures showed improved coverage (as indicated in Table I) and larger values of MIMO capacity (as indicated in Figs. 7 and 8) compared with the slab, especially the effective wall structures.

V. CONCLUSIONS AND DISCUSSIONS

The effect of the complex wall on the path loss prediction, the small-scale fading, and the MIMO capacity are examined using FDTD simulations. It is shown that the patterns of the local mean power distribution for the complex wall cases are quite different from that of the slab and effective wall cases, as shown in Fig. 1. The areas covered by power contours with same power levels are also different by as much as 40% to 50%. The mean values of K factors of complex wall cases are larger than that of the slab walls by around 3 to 5 dB, while the K values of effective walls are larger than the complex wall cases by as large as 7 dB. It is shown that, as the number of Tx and Rx increases, the MIMO capacities increase but at a slower speed than the ideal cases. It is observed that, for each of the three wall structures, larger values of K factors lead to a smaller increase of capacities when the number of antennas increases. It is also shown that the complex wall structures give larger MIMO capacities for most regions except the LOS region where the capacities are similar to that of the slab wall cases. The effective wall structures give the lowest MIMO capacities in all cases. Based on these results, it may be concluded that the complex wall effect on the propagation characteristics and the MIMO capacity could not be appropriately approximated by effective wall structures. These results show that detailed modeling of wall structures is important in the accurate characterization of the fading channel of indoor propagation. Ongoing work involves making similar

calculations for much larger complex propagation environments using ray-tracing codes [23] rather than the FDTD method.

REFERENCES

[1] C. L. Holloway, P. L. Perini, R. R. DeLyser, and K. C. Allen, "Analysis of composite walls and their effects on short-path propagation modeling," *IEEE Trans. Veh. Technol.*, vol. 46, pp. 730–738, Aug. 1997.

[2] M. F. Iskander and Z. Yun, "Propagation prediction models for wireless communication systems," *IEEE Trans. Microwave Theory Tech.*, vol. 50, pp. 662–673, Mar. 2002.

[3] M. F. Iskander, Z. Yun, and Z. Zhang, "Outdoor/indoor propagation modeling for wireless communications systems," in *Dig. IEEE AP-S Int. Symp. USNC/URSI National Radio Science Meeting*, vol. 2, July 8–13, 2001, pp. 150–153.

[4] Z. Zhang, R. K. Sorensen, Z. Yun, M. F. Iskander, and J. F. Harvey, "A ray-tracing approach for indoor/outdoor propagation through window structures," *IEEE Trans. Antennas Propagat.*, vol. 50, pp. 742–748, May 2002.

[5] G. E. Athanasiadou and A. R. Nix, "A novel 3-D indoor ray-tracing propagation model: The path generator and evaluation of narrow-band and wide-band predictions," *IEEE Trans. Veh. Technol.*, vol. 49, pp. 1152–1168, July 2000.

[6] J. T. Zhang and Y. Huang, "Indoor channel characteristics comparison for the same building with different dielectric parameters," in *Proc. IEEE Int. Conf. Commun.*, vol. 2, 2002, pp. 916–920.

[7] D. Chizhik, G. J. Foschini, M. J. Gans, and R. A. Valenzuela, "Keyholes, correlations, and capacities of multielement transmit and receive antennas," *IEEE Trans. Wireless Commun.*, vol. 1, pp. 361–368, Apr. 2002.

[8] C. Chuah, D. N. C. Tse, J. M. Kahn, and R. A. Valenzuela, "Capacity scaling in MIMO wireless systems under correlated fading," *IEEE Trans. Inform. Theory*, vol. 48, pp. 637–650, Mar. 2002.

[9] S. Loyka and A. Kouki, "New compound upper bound on MIMO channel capacity," *IEEE Commun. Lett.*, vol. 6, pp. 96–98, Mar. 2002.

[10] D. Shiu, G. J. Foschini, M. J. Gans, and J. M. Kahn, "Fading correlation and its effect on the capacity of multielement antenna systems," *IEEE Trans. Commun.*, vol. 48, pp. 502–513, Mar. 2000.

[11] A. L. Moustakas, H. U. Baranger, L. Balents, A. M. Sengupta, and S. H. Simon, "Communication through a diffusive medium: Coherence and capacity," *Science*, vol. 287, pp. 287–290, Jan. 2000.

[12] P. E. Driessen and G. J. Foschini, "On the capacity formula for multiple input-multiple output wireless channels: A geometric interpretation," *IEEE Trans. Commun.*, vol. 47, pp. 173–176, Feb. 1999.

[13] G. J. Foschini and M. J. Gans, "On limits of wireless communications in a fading environment when using multiple antennas," *Wireless Personal Commun.*, vol. 6, no. 3, pp. 311–335, Mar. 1998.

[14] G. J. Foschini, "Layered space-time architecture for wireless communication in a fading environment when using multi-element antennas," *Bell Labs Tech. J.*, pp. 41–59, Autumn 1996.

[15] A. F. Molisch, M. Steinbauer, M. Toeltsch, E. Bonek, and R. S. Thoma, "Capacity of MIMO systems based on measured wireless channels," *IEEE J. Select. Areas Commun.*, vol. 20, pp. 561–569, Apr. 2000.

[16] J. Ling, D. Chizhik, P. Wolniansky, R. A. Valenzuela, N. Costa, and K. Huber, "Multiple transmit multiple receive capacity survey in Manhattan," *Electron. Lett.*, vol. 37, no. 16, pp. 1041–1042, Aug. 2001.

[17] H. Xu, M. J. Gans, N. Amitay, and R. A. Valenzuela, "Experimental verification of MTMR system capacity in controlled environment," *Electron. Lett.*, vol. 37, no. 15, pp. 936–937, July 2001.

[18] R. A. Valenzuela, O. Landron, and D. L. Jacobs, "Estimating local mean signal strength of indoor multipath propagation," *IEEE Trans. Veh. Technol.*, vol. 46, pp. 203–212, Feb. 1997.

[19] W. Honcharenko, H. L. Bertoni, and J. Dailing, *Bi-Lateral Averaging Over Receiving and Transmitting Areas for Accurate Measurements of Sector Average Signal Strength Inside Buildings*.

[20] T. S. Rappaport, *Wireless Communications, Principle and Practice*. Upper Saddle River, NJ: Prentice-Hall, 1996.

[21] G. L. Stuber, *Principles of Mobile Communication*, 2nd ed. Norwell, MA: Kluwer, 2001.

[22] F. van der Wijk, S. Kegel, and R. Prasad, "Assessment of a pico-cellular system using propagation measurements at 1.9 GHz for indoor wireless communications," *IEEE Trans. Veh. Technol.*, vol. 44, pp. 155–162, Feb. 1995.

[23] Z. Yun, Z. Zhang, and M. F. Iskander, "A ray-tracing method based on the triangular grid approach and application to propagation prediction in urban environments," *IEEE Trans. Antennas Propagat.*, vol. 50, pp. 750–758, May 2002.

Zhengqing Yun (M'98) received the Ph.D. degree in electrical engineering from Chongqing University, Chongqing, China, in 1994.

He was a Postdoctoral fellow from 1995 to 1997 with the State Key Laboratory of Millimeter Waves, Southeast University, Nanjing, China. From 1997 to 2002, he was with the Electrical Engineering Department, University of Utah, Salt Lake City. He is currently an Assistant Researcher with the Hawaii Center for Advanced Communication, University of Hawaii at Manoa, Honolulu. His recent research interests include development of numerical methods, modeling of radio propagation for wireless communications systems including MIMO, and design and simulation of antennas.

Dr. Yun was the recipient of the 1997 Science and Technology Progress Award (1st Class) presented by The State Education Commission of China.

Magdy F. Iskander (F'93) is the Director of the Hawaii Center for Advanced Communications (HCAC), College of Engineering, University of Hawaii at Manoa, Honolulu. He was a Professor of Electrical Engineering and the Engineering Clinic Endowed Chair Professor at the University of Utah, Salt Lake City, for 25 years. He was also the Director of the Center of Excellence for Multimedia Education and Technology. From 1997 to 1999, he was a Program Director in the Electrical and Communication Systems Division of the National Science Foundation (NSF). At NSF, he formulated and directed a "Wireless Information Technology" initiative in the Engineering Directorate and funded over 29 projects in the microwave/millimeter wave devices, RF MEMS technology, propagation modeling, and the antennas areas. In 1986, he established the Engineering Clinic Program to attract industrial support for projects for undergraduate engineering students and has been the Director of this program since its inception. To date, the program has attracted more than 115 projects sponsored by 37 corporations from across the U.S. The Clinic Program now has an endowment for scholarships and a professorial chair held by the Director at the University of Utah. He spent sabbatical and other short leaves at Polytechnic Institute of New York, Brooklyn; Ecole Superieure D'Electricite, France; the University of California, Los Angeles; Harvey Mudd College, Claremont, CA; Tokyo Institute of Technology, Tokyo, Japan; Polytechnic University of Catalunya, Catalunya, Spain; and at several universities in China. He has published over 170 papers in technical journals, has nine patents, and has made numerous presentations in technical conferences. He authored the textbook *Electromagnetic Fields and Waves* (Englewood Cliffs, NJ: Prentice-Hall, 1992), and he edited the CAEME Software Books (Vol. I, 1991 and Vol. II, 1994) and four other books on the microwave processing of materials (Materials Research Society, 1990–1996). He edited four special issues of journals including two for the *Journal of Microwave Power* and a special issue of the *ACES Journal*. He also edited the 1995 and 1996 proceedings of the *International Conference on Simulation and Multimedia in Engineering Education*. His ongoing research contracts include "Propagation Models for Wireless Communication" and "Low-Cost Phased Array Antennas," both funded by the Army Research Office and NSF, "Electronically tunable microwave devices," funded by Raytheon, "Microwave Processing of Materials," funded by Corning, Inc., and the "Conceptual Learning of Engineering" funded by NSF.

Dr. Iskander received the 1985 Curtis W. McGraw ASEE National Research Award, the 1991 ASEE George Westinghouse National Education Award, the 1992 Richard R. Stoddard Award from the IEEE EMC Society, the 2000 University of Utah Distinguished Teaching Award, and he is the founding Editor of the journal *Computer Applications in Engineering Education*, which received the Excellence in Publishing award in 1993. He was a member of the WTEC panel on "Wireless Information Technology" and the Chair of the Panel on "Asia Telecommunications" sponsored by the DoD and organized by the International Technology Research Institute (ITRI) from 2000 to 2001. As part of these studies, he visited many wireless companies in Europe, Japan, and several telecommunications institutions and companies in Taiwan, Hong Kong, and China. He was a member of the National Research Council Committee on Microwave Processing of Materials. He organized the first "Wireless Grantees Workshop" sponsored by NSF and held at the National Academy of Sciences in 2001. He was the 2002 President of the IEEE Antennas and Propagation Society (APS), the Vice President in 2001, and he was a member of the IEEE APS AdCom from 1997 to 1999. He was the General Chair of the 2000 IEEE APS Symposium and URSI meeting, Salt Lake City, UT, and was a Distinguished Lecturer for the IEEE APS from 1994 to 1997. He edited the special issue of the IEEE TRANSACTIONS ON ANTENNAS AND PROPAGATION, May 2002, which included contributions from NSF-funded projects. While serving as a distinguished lecturer for the IEEE, he has given lectures in Brazil, France, Spain, China, Japan, and at a large number of U.S. universities and IEEE chapters.

Zhijun Zhang (M'00) received the B.S. and M.S. degrees in electrical engineering from the University of Electronic Science and Technology of China, Chengdu, in 1992 and 1995, respectively, and the Ph.D. degree in electrical engineering from Tsinghua University, Beijing, China, in 1999.

From 1999 to 2001, he was a Postdoctoral Fellow with the Department of Electrical Engineering, University of Utah, Salt Lake City. He was appointed a Research Assistant Professor in same the Department in 2001. He was with the University of Hawaii at Manoa, Honolulu, in 2002, where he was an Assistant Researcher.